Femtosecond Fluorescence Dynamics of *trans*-Azobenzene in Hexane on Excitation to the $S_1(n,\pi^*)$ State

Ying-Chih Lu (盧盈志), Chih-Wei Chang (張智煒) and Eric Wei-Guang Diau* (刁維光)
Department of Applied Chemistry, National Chiao Tung University, Hsinchu, Taiwan 30050, R.O.C.

Femtosecond fluorescence dynamics of *trans*-azobenzene in hexane have been investigated on excitation to the $S_1(n,\pi^*)$ state at 432 nm using the up-conversion technique. Two transient components were observed to represent the fast and the slow S_1 fluorescence dynamics in the wavelength range of 550-732 nm. Based on the results obtained from recent *ab initio* calculations (Ishikawa, T.; Noro, T.; Shoda, T., *J. Chem. Phys.* **2001**, *115*, 7503), a dynamical picture is given in the following. Upon initial excitation to the S_1 state, the excited molecule is moving away from the first detection window within the observed 200-300 fs. The structural relaxation from the Franck-Condon region may be responsible for the observed fast S_1 dynamics with the driving force being the CNNC twisting motion along the rotational coordinate. For the rest of the motion on the S_1 global potential surface, the excited molecule may search for the S_0/S_1 conical intersection for an efficient internal conversion to the ground state. The nuclear motions for the observed slow S_1 dynamics not only involve the CNNC torsional coordinate but also the other degrees of freedom such as the CNN bending coordinate on the multidimensional S_1 potential energy surface. The whole electronic relaxation process occurs within the observed 1-2 ps. The slow S_1 dynamics were found to vary with the fluorescence wavelengths due to the influence of the solvent-induced vibrational relaxation in the S_1 state; the vibrational relaxation should occur on a time scale comparable to the time scale of the electronic relaxation ($S_1 \rightarrow S_0$ internal conversion).

INTRODUCTION

The *cis*-*trans* photoisomerization of azobenzene and its derivatives has been a subject for many years for its potential industrial applications in light-triggered optical switches and memory-storage devices.[1-7] From a fundamental viewpoint, photo-excitation of the azobenzene molecules into their electronic excited states leads to isomerization which gives the ground-state products with both *trans*- and *cis*-conformations. However, the mechanism for the *cis*-*trans* photoisomerization of azobenzene still remains ambiguous according to recent investigations.[8-11]

The steady-state UV-visible spectra of both azo-isomers in solutions are featured with two absorption bands that respectively represent the $S_0 \rightarrow S_1$ and the $S_0 \rightarrow S_2$ transitions.[7,9,12-14] In the visible region, the $S_0 \rightarrow S_1$ transition corresponds to a perpendicular electronic excitation from the non-bonding n orbital of the N atom to the anti-bonding π^* orbital with the maximum intensity near 440 nm for both isomers. For the *trans*-isomer with C_{2h} symmetry, this electronic transition ($\tilde{A}^1B_g \leftarrow \tilde{X}^1A_g$) is strictly forbidden.[9] However, for the *cis*-isomer with C_{2v} symmetry, the electronic transition ($\tilde{A}^1B_1 \leftarrow \tilde{X}^1A_1$) is symmetry allowed.[7] Such a symmetry discrepancy between *trans*- and *cis*-azobenzenes gives the maximum intensity of the *cis*-isomer greater than that of the *trans*-isomer by almost a factor of three.[7,15,16] In the UV region, the $S_0 \rightarrow S_2$ transition corresponds to the symmetry-allowed $\pi-\pi^*$ transition with the maximum intensity near 320 nm and 280 nm for *trans*- and *cis*-isomers, respectively. The spectral feature of the $S_0 \rightarrow S_2$ transition of azobenzene is similar to that of the $\pi-\pi^*$ transition of stilbene – a similar molecule with pivotal C=C double bond instead of the N=N double bond.[17-20]

Early steady-state measurements show that the isomerization quantum yields for the $S_0 \rightarrow S_1$ transition and the $S_0 \rightarrow S_2$ transition are different – the *trans*-to-*cis* quantum yields are 0.23 and 0.10 for the former and the latter, respectively, indicating different isomerization mechanisms may be operating upon excitations into different electronic excited states.[7] Based on Rau and Lüddecke's results[8] showing almost the same *trans*-to-*cis* quantum yields (0.24 vs. 0.21) for the azobenzene derivatives of which the free rotation about the N=N double bond is prohibited, two possible photoisomerization mechanisms are proposed:[7,8,21] Visible excitation to the $S_1(n,\pi^*)$ state may lead to the isomerization via inversion around one nitrogen atom in the same molecular plane

Dedicated to the celebration of the seventieth anniversary of Chemical Society the located in Taipei.

whereas UV excitation to the $S_2(\pi,\pi^*)$ state may result in the isomerization via the rotation around the N=N double bond. This mechanism has been widely accepted by recent time-resolved studies,[15,21-24] and the relevant results will be described in the following.

In recent years, many ultrafast spectroscopic experiments were carried out in solutions to justify the proposed photoisomerization mechanism for azobenzene excited to the $S_1(n,\pi^*)$ and the $S_2(\pi,\pi^*)$ states.[11,15,16,21-25] Because the $S_0 \rightarrow S_2$ transition is the strongest absorption band, studies on the S_2 dynamics of azobenzene are relatively rich. The first femtosecond (fs) study of the system was reported by Lednev et al.[23] using transient UV-visible absorption spectroscopy technique on excitation of *trans*-azobenzene at 303 nm and detection at 370-450 nm. The observed short-lived component with time constant $\tau \sim 1$ ps was attributed to the S_2 species and a longer time scale component ($\tau = 11$-15 ps) was assigned to a twisted conformer on the S_2 or S_1 potential energy surface (PES). It is worth noting that the partial recovery time of the ground-state absorption at 303 nm is 13 ps, which makes the authors give an alternative interpretation for the long component – it is due to vibrational relaxation of hot *trans*-azobenzene molecules in the ground state. This vibrational relaxation model has been supported by two other recent time-resolved investigations. First, combining fs transient IR spectroscopy technique and model calculations, the time scale for the solvent-induced intermolecular vibrational relaxation was reported to be ~20 ps.[16] Second, using picosecond (ps) Raman spectroscopy technique, the lifetime of vibrationally excited S_0 azobenzene was determined to be ~16 ps via analysis of the anti-Stokes NN stretch band.[22] In fact, in a subsequent letter Lednev et al.[24] revised their interpretation based on the results obtained with better time resolution (see below).

Two relevant results upon excitation to the $S_1(n,\pi^*)$ state are summarized as follows. Using fs transient absorption technique, Nägele et al.[15] studied the S_1 photoisomerization dynamics of azobenzenes at 435 nm and found two transient components for both *trans* and *cis* isomers – the fast component (with time constants of 170 fs and 320 fs for the *cis*- and the *trans*-isomers, respectively) was assigned to be due to the isomerization process and the slow component (~2 ps for both isomers) due to a "diffusion-type" motion on the S_1 potential surface. Using the same experimental technique to study the S_1 photoisomerization dynamics of *trans*-azobenzene on excitation at 390 nm, 420 nm, and 503 nm, Lednev et al.[24] reported the fast transient component with a time constant of ~0.6 ps and the slow component of 2.5 ps. Since the fast component was not observed at the longest excitation wavelength (503 nm), a different assignment for the S_1 dynamics of azobenene was therefore proposed: the slow 2.5 ps component is due to the *trans*-to-*cis* isomerization process and the additional fast sub-ps component may arise from vibrational relaxation.

Despite the very low fluorescence quantum yield for both $S_0 \rightarrow S_1$ and $S_0 \rightarrow S_2$ excitations of *trans*-azobenzene, the fs time-resolved fluorescence measurements have been carried out by Fujino et al.[11] with the photo-excitation at 280 nm and the fluorescence detection at 380-640 nm. The lifetimes of the S_2 and the S_1 states were determined to be ~110 fs and ~500 fs, respectively. The quantum yield for the $S_2 \rightarrow S_1$ electronic relaxation was found to be almost unity, suggesting that the isomerization following S_2 excitation should take place in the S_1 state and a sequential mechanism ($S_2 \rightarrow S_1^{\dagger} \rightarrow S_0^{\dagger\dagger}$, where † and †† represents the excess vibrational energies for the S_1 and S_0 species, respectively) is established. Compared to the results obtained from the transient absorption technique, the observed much shorter lifetime (500 fs vs. 2.5 ps) for the S_1 fluorescence dynamics may be due to the much larger excess vibrational energy in the $S_1^{\dagger}$ species upon excitation at 280 nm with respect to the previous transient absorption experiments on excitation at 503 nm. However, the sequential mechanism is inconsistent with the commonly accepted mechanism of Rau and Lüddecke.[7,8] Therefore, "the opening of a new relaxation channel that is related to the rotational coordinate" has been proposed.

Because of the relatively large size of the azobenzene molecule, theoretical studies[10,26-29] for characterization of the excited-state PESs along the inversion and the rotation coordinates have not been practical until recently. Early *ab initio* work of Monti et al.[26] based on minimal basis set CI calculations should only give a qualitative picture to describe the photochemistry of azobenzene; however, their results have been widely adopted in many experimental studies to explain the dual isomerization mechanism that Rau and Lüddecke have proposed. Using more advanced methods such as CASSCF and CIPSI with a larger basis set, Cattaneo and Persico[27] do obtain the excited-state potential energy curves of azobenzene that are indeed in many aspects significantly different from those of Monti et al.[26] Recently, Ishikawa et al.[10] have carried out two-dimensional surface-scan calculations for the S_0, $S_1(n,\pi^*)$, $S_2(\pi,\pi^*)$ and $S_3(n^2,\pi^{*2})$ states of azobenzene using high-level CASSCF and MRCISD methods. Both recent high-level *ab initio* results have shown that the S_1 PES of *trans*-azobenzene involves a substantial energy barrier along the inversion coordinate, but it is essentially barrierless along the rotational coordinate. Furthermore, the results of Ishikawa et al. also indicate that a conical intersec-

tion (CI) between the S_0 and the S_1 states is located near the midpoint of the rotation pathway, which suggests that the photoisomerization of azobenzene on the S_1 surface may favor the rotation mechanism from a theoretical point of view.

Apparently, the dual photoisomerization mechanism of azobenzene is challenged by both recent experimental study[11] and theoretical investigations[10,27] and the rotation vs. inversion controversy[7] has not been resolved yet. Since time-resolved florescence spectroscopy has the advantage of a well-defined detection window between the target excited state and the ground state, it may provide very important dynamical information for the understanding of the photochemistry of azobenzene in solution. A previous fs fluorescence study of Fujino et al.[11] was performed on excitation to the S_2 state; therefore, the information corresponding to the S_1 dynamics was inferred indirectly from the data obtained at longer fluorescence wavelengths. In this work, we carried out fs fluorescence up-conversion measurements for investigation of the photoisomerization dynamics of *trans*-azobenzene in nonpolar solvent upon excitation *directly* into the $S_1(n,\pi^*)$ state (λ_{ex} = 432 nm). The up-conversion signal was detected in a broad fluorescence wavelength range (λ_{fl} = 550-732 nm) and the results with respect to the S_1 photoisomerization dynamics are discussed.

EXPERIMENT

The time-resolved fluorescence measurements were performed using a fs optically gated system (FOG-100, CDP); the experimental setup is schematically shown in Fig. 1. The fs light source is a broadband mode-locked Ti:sapphire laser (Mira 900D, Coherent) pumped by a 10 W Nd:YVO_4 laser (Verdi-V10, Coherent). The oscillator generates a 76 MHz pulse train with 0.5-1.8 W average power in a tunable range of 700-980 nm. In the present study, the center wavelength of the fs pulse was fixed at 864 nm with average power ~1.3 W. The spectral characteristic of the pulse was measured by an ultrafast laser spectrum analyzer (E201, REES); the pulse spectrum has FWHM ~12 nm at 864 nm. The temporal characteristic of the pulse was determined by an autocorrelator (Mini, APE); the autocorrelation of the pulse gives a temporal profile with FWHM ~140 fs (pulse duration ~100 fs) at 864 nm.

The pulses were focused onto a 0.5 mm-thick BBO type-I nonlinear crystal (NC1; Fig. 1) for the second harmonic generation (SHG; Fig. 1). The second harmonic pulses were separated from the fundamental pulses with a dichroic beam splitter (BS; Fig. 1) and used as pump pulses. The pump pulses were focused onto a 1 mm-thick rotating cell (SC; Fig. 1) containing sample solutions. The fluorescence emitted from the sample was collected by a lens pair (AL and L4; Fig. 1) and focused on another BBO type-I crystal (NC2; Fig. 1). The optically delayed fundamental pulses were also focused on NC2 and used as gate pulses for sum-frequency generation (SFG; Fig. 1). The fluorescence and the gate pulse interact non-collinearly in NC2, and typically the crossing angle between the two beams is about 5°. The fluorescence wavelength to be up-converted by SFG was selected by changing the phase-matching angle of NC2. The sum-frequency signal was spatially and spectrally separated from the other interfering lights (such as fluorescence itself, the gate pulse, and the unphase-matched SHG due to the intense gate pulse) by a combination of an iris, a band-pass filter (F3; Fig. 1), and a single monochromator (CDP2022). The width for the entrance and exit slits of the monochromator was kept at 1.0 mm, which gives the spectral resolution of 8.7 nm at λ = 300 nm. The signal was detected via a photon-counting PMT (R1527P, Hamamatsu) and then transferred to a PC through RS-232 interface (represented by dotted arrowed lines in Fig. 1) for data acquisition and manipulations. By varying the delay time between the excitation pulse and the gate pulse through the optical delay line, the transient profiles were obtained.

A Berek's variable waveplate (BW; Fig. 1) was used as

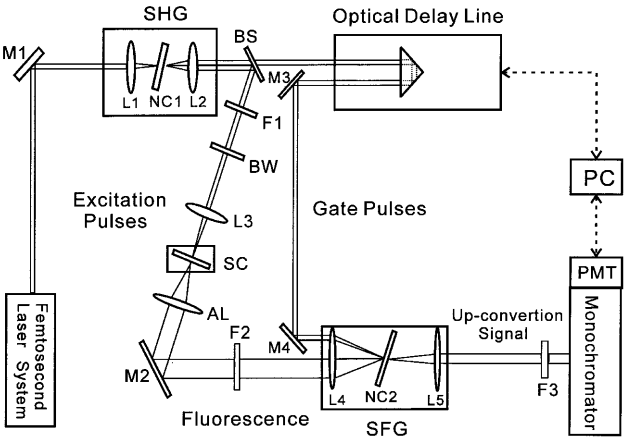

Fig. 1. Experimental setup used for the femtosecond fluorescence up-conversion measurements. M1-M4: mirrors; L1-L5: lenses; F1-F3: optical filters; NC1-NC2: nonlinear crystals; BS: dichroic beam splitter; BW: Berek's variable waveplate; SC: rotating sample cell; AL: achromatic lens; SHG: second-harmonic generation; SFG: sum-frequency generation; PMT: photomultiplier tube; PC: personal computer.

a λ/2 plate to change the polarization of the excitation pulses for the time-dependent anisotropy measurements. In the present study the pump-probe polarization was set at the parallel configuration in order to get the best signal-to-noise ratio for the SFG signal converted from the extremely weak fluorescence emission. Therefore, both rotational and tilted angles of BW were adjusted to reach the maximum intensity for the third harmonic generation (THG) signal at the parallel polarization of the pump (SHG) pulse with respect to the probe (fundamental) pulse.

The current photon-counting detection system has a very high duty cycle because the fs oscillator is operated at a very high repetition rate (7.6×10^7 shots per second). To avoid saturation effect and the overflow damage of the detector, the THG signal was always kept below 10^6 counts per second via attenuation of the incident fs intensity using an appropriate neutral-density filter. In the present study, it has been recognized that the fluorescence of *trans*-azobenzene resulting from the S_1 state is normally non-observable in a typical steady-state measurement due to its very low fluorescence quantum yield. Therefore, we were struggling in the first stage for the optical alignment to find the weak signal for the title molecule. To overcome this problem, a laser dye emitting fluorescence with high enough efficiency in a similar wavelength region was used for initial alignment. We have chosen DCM dye for this purpose. For each transient, typically a total of 300 data points were taken in three different time intervals (100 points each) depending on the composition and the corresponding lifetime of the transient, with 6-9 seconds of accumulating time for each data averaging. To examine the contributions from the multiphoton excitation processes, a test for the power dependence of the pump pulse was performed. The results indicate that the up-conversion signal is indeed due to a one-photon excitation process under the current experimental conditions.

Experimental data were analyzed with an appropriate kinetic model (see below) including convolution of the laser pulses. Two important parameters, time zero and instrumental response function (IRF), should be precisely determined in order to extract the kinetics (in particular with a fast-decay component of which the lifetime is comparable to the FWHM of the laser pulse) from deconvolution.[30] Both time zero and the FWHM of IRF were treated as free parameters in our non-linear curve fitting procedure because these two parameters strongly depend on the probing wavelength due to the group velocity dispersion (GVD) arising from the lens pair used to collect the fluorescence. Fig. 2 shows the substantial effect of GVD shifting the time zero at five different fluorescence wavelengths – 550 nm, 607 nm, 643 nm, 687 nm, and 732 nm; all five measurements were performed with the starting point at exactly the same delay time. Since the fluorescence at 550 nm suffers more GVD than the fluorescence at 732 nm, the time zero at 550 nm is delayed by almost 1 ps compared to the time zero at 732 nm. The IRF was also substantially affected by GVD at various fluorescence wavelengths, which will be further discussed in the next section. The present test indicates that one must consider the influence of GVD leading to the time zero shift and the variation of the instrument response in analyzing the transient data, particularly for those fs time-resolved spectra taken via the CCD spectrometer.

Trans-azobenzene (99%) was purchased from Aldrich and used without further purification. The samples were dissolved in hexane (HPLC grade). The transient response from the sample was identical in the concentration range of 1×10^{-3} mol L^{-1} – 1×10^{-2} mol L^{-1}. For all experimental data reported in this paper, the sample concentration is 5.0×10^{-3} mol L^{-1}.

RESULTS AND DISCUSSION

The Kinetic Model

The temporal characteristic of the pulse (instrumental response function) at the excitation wavelength of 432 nm is

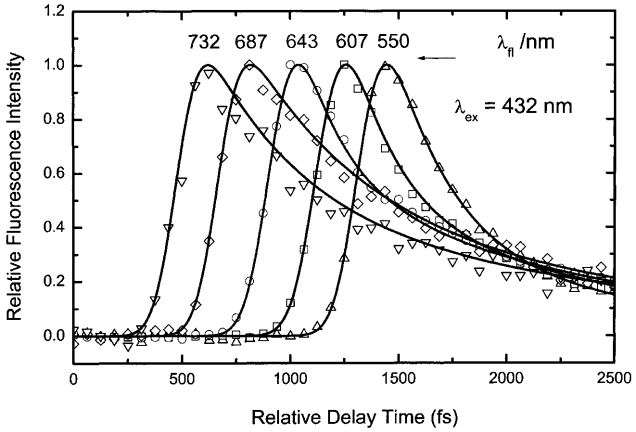

Fig. 2. Time-resolved fluorescence signals of *trans*-azobenzene in hexane obtained from five different fluorescence wavelengths as indicated. The same starting point of the delay time between pump and probe pulses was applied for each transient. The substantial time zero shifts for the transients between the longer wavelengths and the shorter wavelengths were due to the effect of group velocity dispersion (GVD) imposed on different wavelengths (see text).

assessed from the temporal profile of the THG signal, which can be fitted to a Gaussian function with the FWHM equal to ~220 fs (Fig. 3A). When the probing wavelength was tuned to the region where the fluorescence can be effectively up-converted, the transients for the S_1 photoisomerization dynamics of *trans*-azobenzene in hexane were collected. A typical transient trace is shown in Fig. 3B. Since the "spike-like" component in the transient cannot be described solely by an IRF, a simple consecutive kinetic model is therefore employed to account for the observed temporal profile:

$$A \xrightarrow{\tau_1} B \xrightarrow{\tau_2} C \qquad (1)$$

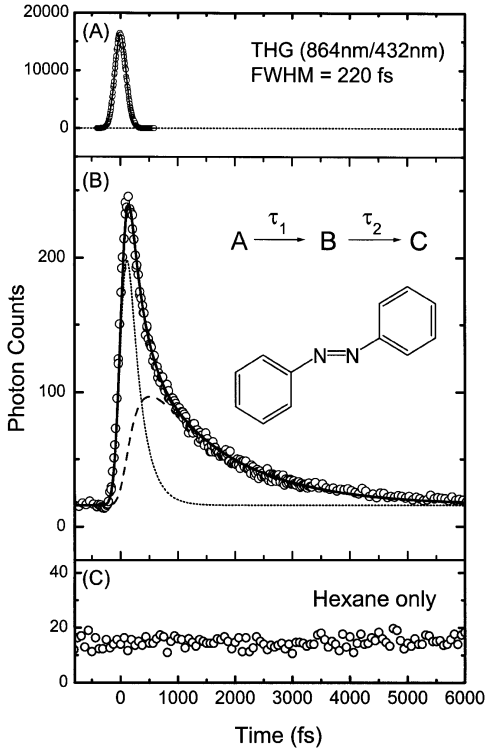

Fig. 3. (A) The THG signal obtained from the SFG measurement between the fundamental pulse (864 nm) and the SHG pulse (432 nm). The FWHM of the THG is ~220 fs. (B) A typical transient of *trans*-azobenzene in hexane at λ_{ex} = 432 nm showing the bi-exponential feature that is described by a consecutive kinetic model with the corresponding time constants as indicated. The dotted curve represents the fast transient component A and the dashed curve represents the slow transient component B. (C) The blank experiment with hexane only in the sample cell showing only the background (dark) signal.

where the fast component A is described by a single exponential function with a decay time constant τ_1 and the slow component B described by a bi-exponential function with a rise time constant τ_1 and a decay time constant τ_2. To further make sure that the initial fast decay component A is not due to the unphase-matched THG interference in the same detection window, a blank experiment was performed in the same sample cell containing only the hexane solvent. The result obtained from the blank experiment (Fig. 3C) has confirmed that both fast and slow components shown in Fig. 3B are genuinely arising from the emission of the electronically excited *trans*-azobenzene.

The transients taken at five different fluorescence wavelengths are shown in Fig. 4. For each trace, the two resolved components represent A and B in model (1) with the corresponding time constants fitted according to this consecutive kinetic model. Fig. 5 shows these five transients to-

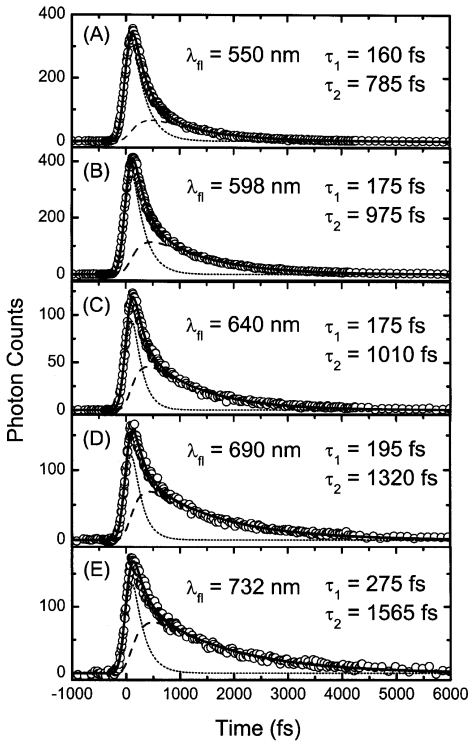

Fig. 4. Fluorescence up-conversion signals of *trans*-azobenzene in hexane on excitation at λ_{ex} = 432 nm with the fluorescence wavelengths observed at (A) 550 nm; (B) 598 nm; (C) 640 nm; (D) 690 nm; (E) 732 nm. The time constants shown for each transient were obtained by a non-linear curve fitting procedure with convolution of laser pulses according to the kinetic model described in the text.

gether with the fitted curves normalized in a short time range to further extend the vision for the rising part of the transient, which is predominantly characterized by IRF. As mentioned in the experimental section, the zero delay time and the instrumental FWHM were set as free parameters when fitting the data. The delay of time zero due to GVD at various wavelengths has been demonstrated in Fig. 2. After the correction for the time zero shift, the effect of IRF broadening due to GVD is illustrated in Fig. 5; the transients shown from the top to the bottom curves were taken at the wavelengths of 550 nm, 598 nm, 640 nm, 690 nm, and 732 nm, respectively. The value of FWHM was fitted to decrease gradually from 250 fs at 550 nm to 190 fs at 732 nm because the fluorescence at a shorter wavelength suffers more GVD than the fluorescence at a longer wavelength.

The Fast S_1 Dynamics

Because all the transient signals shown in Fig. 4 decay to the background level at longer times (>10 ps, not shown), no other long-lived fluorescence state except the fast-decay component A and the slow-decay component B was considered to interpret the photoisomerization dynamics of azobenzene. A dynamical model is schematically shown in Fig. 6 to illustrate the S_1 relaxation processes for components A and B according to our experimental findings. Since the excited molecule has the same molecular geometry as the ground-state species upon initial excitation to the S_1 state, it is reasonable to assume that the fast component A is due to the S_1 species in the Franck-Condon (FC) region undergoing initial structural change along the reaction coordinate (RC) toward the S_1 minimum region. The structural relaxation time (τ_1) was fitted to be 160 fs at 552 nm, and it increases only slightly with the wavelength increasing up to 690 nm. For the transient measured at 732 nm, a larger τ_1 value (= 275 fs) was obtained from the standard fitting procedure. If the fitting was made with a constant value of τ_1 = 200 fs, a fit with similar quality of Fig. 4E can be obtained by increasing the FWHM to ~200 fs; the fit was not sensitive to the value of τ_2. Although the larger change in τ_1 at 732 nm is within our experimental uncertainty, it may also suggest that there is a fast intramolecular vibrational relaxation affecting the observed initial S_1 photoisomerization dynamics of azobenzene in solution (see below).

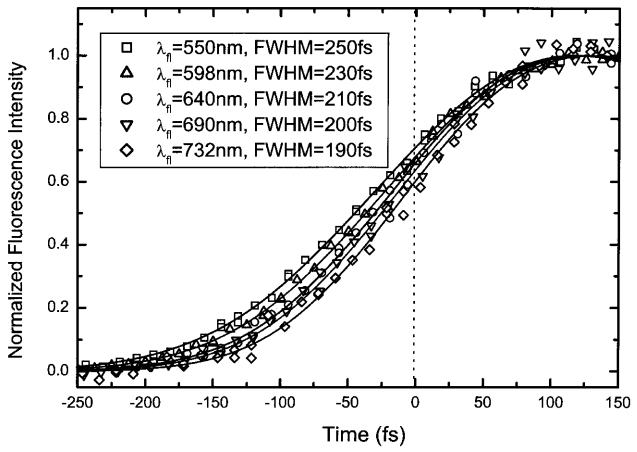

Fig. 5. The combined plot of five transients of Fig. 4 normalized in a short time range to show a systematic GVD broadening effect at various fluorescence wavelengths.

The Slow S_1 Dynamics and Vibrational Relaxation

For the assignment of component B, two dynamical features must be considered in the following. First, the amplitude ratio of A with respect to B gradually decreases from 550 nm to 732 nm. Second, the value of τ_2 shows a dramatic systematic change from the shorter wavelength (τ_2 = 785 fs at 550 nm) to the longer wavelength (τ_2 = 1565 fs at 732 nm). After initial FC relaxation, component B becomes more important at longer wavelengths (fluorescing in lower energy), indicating that B is the observed excited-state species in the S_1 minimum region because the energy difference between the two fluorescing states is small enough to favor the detection at a longer wavelength. This observation is conceptually illustrated in Fig. 6. Therefore, we assign component B to be the excited-state species moving on the S_1 PES along the RC to search for the S_0/S_1 CI, where the energy gap between the S_1 and the S_0 states is essentially zero. After reaching the S_0/S_1 CI, the excited-state species becomes a hot ground-state species and the fluorescence signal is no longer observed.

The observed systematic change in τ_2 on the ps time

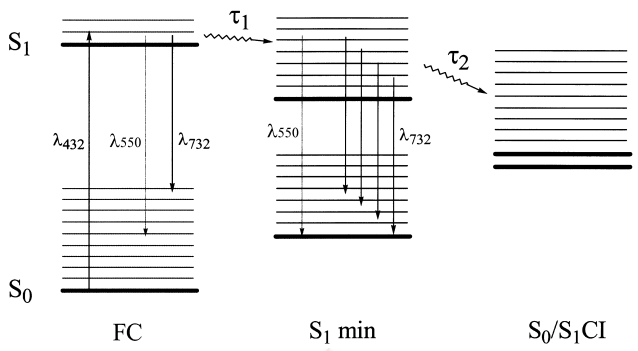

Fig. 6. A dynamical model for interpretation of the observed S_1 fluorescence dynamics of *trans*-azobenzene in solution (see text).

scale further suggests that there should be a relaxation process responsible for the even slower dynamics at longer wavelengths. Such an observation may be explained with the involvement of the solvent-induced vibrational relaxation process that brings the excited species from the highly excited vibrational levels into the lower vibrational levels on the S_1 surface before reaching the S_0/S_1 CI. As shown in Fig. 6, because the "shrinkage" of the energy gap between the S_0 and the S_1 states, the detection window at 550 nm becomes too "narrow" to probe the S_1 populations at the lower vibrational levels. The observed 785 fs at 550 nm is therefore the measured lifetime for the S_1 species at higher vibrational levels undergoing either the solvent-induced relaxation to the lower vibrational levels of the S_1 state or internal conversion to the highly excited vibrational levels of the S_0 state (both are dark at 550 nm). On the other hand, the S_1 species populated at the lower vibrational levels may be observed with the detection window opened at longer wavelengths (Fig. 6). The $S_1 \rightarrow S_0$ internal conversion process is slower at lower vibrational levels because less internal energy is available to search for the S_0/S_1 CI in the multidimensional S_1 PES. Therefore, the observed much longer lifetime (τ_2 = 1565 fs) at 732 nm is due to the wide opening of the detection window at the longer wavelength so that the S_1 populations at the lower vibrational levels can be probed as well. This may be the consequence of the solvent-induced vibrational relaxation affecting the overall S_1 photoisomerization dynamics of azobenzene in solution.

The Comparison with Other Real-Time Investigations

Qualitatively, our results are similar to those of Nägele et al.[15] and those of Lednev et al.;[24] both found two transient components at similar excitation wavelengths using femtosecond transient absorption technique. However, the time constants of both components measured by the transient absorption method are generally larger than what we have observed using the fluorescence up-conversion method. This may be due to a broader detection window involved for the former than the latter. According to the observed systematic trend for the increase of τ_1 and τ_2 at longer fluorescence wavelengths where the detection window is broader, our results are totally consistent with those obtained from the transient absorption measurements,[15,24] by which τ_1 = 0.3-0.6 ps and τ_2 = 2.1-2.6 ps were given. The observed vibrational relaxation process in the S_1 state must occur on a similar time scale in order to compete with the isomerization process taking place on the S_1 PES. In fact, the vibrational cooling of the hot ground-state species was observed to occur on the time scale of 10-20 ps using various ultrafast techniques.[15,16,22-24]

The fast component observed in the transient absorption measurements was previously suggested to arise from the vibrational relaxation because it was absent on excitation at 503 nm.[24] Our results have ruled out this possibility because the vibrational relaxation process cannot be completed within the time scale of the fast-decay component and it has significantly affected the slow S_1 dynamics at longer times. On the other hand, our assignment for the fast-decay component to be the initially excited molecule moving away from the FC region is consistent with the result of Lednev et al.[24] without seeing this fast component at 503 nm because the transition probability between the S_1 and S_n states in the FC region may be too small to be observed in the transient absorption measurements.

Fujino et al.[11] have measured the fluorescence dynamics of *trans*-azobenzene upon excitation to the $S_2(\pi,\pi^*)$ state with λ_{ex} = 280 nm. The transients observed at the fluorescence wavelengths similar to ours (λ_{fl} = 560 nm and λ_{fl} = 640 nm) show clearly a bi-exponential kinetic feature, and they have analyzed the lifetimes to be pulse-limited and ~500 fs for the fast and the slow components, respectively. On excitation directly into the $S_1(n,\pi^*)$ state with λ_{ex} = 432 nm, we observed τ_2 = 1010 fs at λ_{fl} = 640 nm. Although our result is slower than that of Fujino et al. by a factor of two at the same detection wavelength, the available energy in their measurements is much higher than ours. As a result, a much slower S_1 fluorescence dynamics was observed in our study.

CONCLUDING REMARKS

Using the technique of femtosecond fluorescence up-conversion spectroscopy, we have carried out real-time measurements to study the photoisomerization dynamics of *trans*-azobenzene in hexane upon direct excitation to the symmetry-forbidden $S_1(n,\pi^*)$ state. The transient signals show an apparent bi-exponential character that can be fitted into our consecutive kinetic model with two distinct components. From the experimental viewpoint, our real-time observation did not provide structural evidence for judging the S_1 photoisomerization mechanism of azobenzene to proceed along either the rotation or the inversion RC. However, the observed "dual-fluorescence" dynamics are consistent with the theoretical results obtained from recent high-level *ab initio* calculations.[10,27] Because the S_1 minimum and the S_0/S_1 CI are located in the middle of the rotational pathway, we summarize the results of Ishikawa et al.[10] in Fig. 7 to demon-

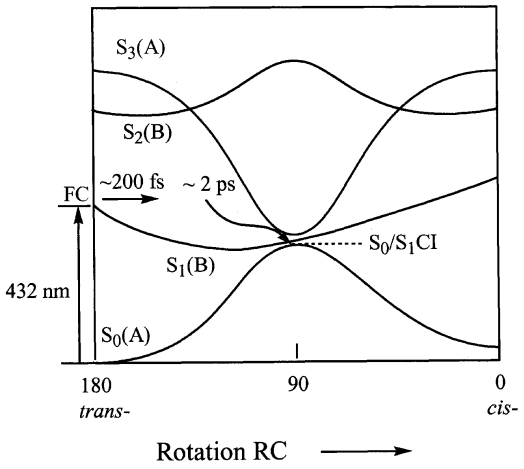

Fig. 7. A dynamical picture conceptually showing the S_1 isomerization dynamics of azobenzene on a multidimensional potential energy surface along the rotational coordinate (see text).

strate the observed S_1 dynamics of azobenzene along the rotation RC. Upon excitation to the S_1 state at λ_{ex} = 432 nm, the excited molecule is moving away from the FC region toward the S_1 minimum region within the observed 200-300 fs along the rotation RC (the source of component A). The S_1 minimum has a rotamer structure with the CNNC torsional angle of 125°-135° according to Ishikawa et al.[10] and Cattaneo and Persico.[27] Ishikawa et al.[10] have further located the structure for the S_0/S_1 CI to have a perpendicular geometry with the CNNC torsional angle of 88° and the CNN bending angle as wide as 130°. Therefore, the observed slower dynamics for component B is due to the nuclear motion on the multidimensional S_1 surface to look for the S_0/S_1 CI along not only the rotation RC but also the other relevant degrees of freedom such as the CNN bending coordinate. The whole process of searching for the S_0/S_1 conical intersection occurs within the observed ~2 ps. The solvent-induced vibrational relaxation taking place in the S_1 state was found to have a time scale comparable to the time scale of the photoisomerization of *trans*-azobenzene on the S_1 potential energy surface.

ACKNOWLEDGMENTS

The femtosecond laser equipment and the fluorescence up-conversion spectrometer were purchased through a starting fund provided by the Center for Interdisciplinary Molecular Science of National Chiao-Tung University. This work was supported by the National Science Council of the Republic of China with the project contract number of 90-2119-M-009-001. We thank Dr. Juen-Kai Wang and Prof. Po-Yuan Cheng for many illuminating discussions. The assistance for the initial setup of the FOG-100 system by Mr. Evgueni of CDP Corp. is gratefully acknowledged.

Received July 15, 2002.

Key Words

Azobenzene; Conical intersection; Femtochemistry; Up-conversion; Photochromism.

REFERENCES

1. Ikeda, T.; Tsutsumi, O. *Science* **1995**, *168*, 1873.
2. Liu, Z. F.; Hashimoto, K.; Hujishima, A. *Nature* **1990**, *347*, 658.
3. Willner, I.; Rubin, S.; Riklin, A. *J. Am. Chem. Soc.* **1995**, *113*, 3321.
4. Sekkat, Z.; Dumont, M. *Appl. Phys. B: Photophys. Laser Chem.* **1992**, *54*, 485.
5. Sudesh, G.; Neckers, D. C. *Chem. Rev.* **1989**, *89*, 1915.
6. Tamai, N.; Miysaka, H. *Chem. Rev.* **2000**, *100*, 1875.
7. Rau, H. In *Photochromism: Molecules and Systems* (Eds: Durr, H.; Bouas-Laurent, H.), Elsevier, Amsterdam, **1990**, pp.165.
8. Rau, H.; Lüddecke, E. *J. Am. Chem. Soc.* **1982**, *104*, 1616.
9. Biswas, N.; Umapathy, S. *Chem. Phys. Lett.* **1995**, *236*, 24.
10. Ishikawa, T.; Noro, T.; Shoda, T. *J. Chem. Phys.* **2001**, *115*, 7503.
11. Fujino, T.; Arzhantsev, S. Y.; Tahara, T. *J. Phys. Chem. A* **2001**, *105*, 8123.
12. Rau, H. *J. Photochem.* **1984**, *26*, 221.
13. Rau, H.; Yu-Quan, S. *J. Photochem. Photobiol. A* **1988**, *42*, 321.
14. Siampringue, N.; Guyot, G.; Monti, S.; Bortollus, P. *J. Photochem.* **1987**, *37*, 185.
15. Nägele, T.; Hoche, R.; Zinth, W.; Wachtveitl, J. *Chem. Phys. Lett.* **1997**, *272*, 489.
16. Hamm, P.; Ohline, S. M.; Zinth,W. *J. Chem. Phys.* **1997**, *106*, 519.
17. Sension, R. J.; Repinec, S. T.; Szarka, A. Z.; Hochstrasser, R. M. *J. Chem. Phys.* **1993**, *98*, 6291.
18. Myers, A. B.; Mathies, R. A. *J. Chem. Phys.* **1984**, *81*, 1152.
19. Waldeck, D. H. *Chem. Rev.* **1991**, *91*, 415.
20. Baskin, J. S.; Banares, L.; Pedersen, S.; Zewail, A. H. *J. Phys. Chem.* **1996**, *100*, 11920.
21. Lednev, I. K.; Ye, T. Q.; Abbott, L. C.; Hester, R. E.; Moore, J. N. *J. Phys. Chem. A* **1998**, *102*, 9161.
22. Fujino, T.; Tahara, T. *J. Phys. Chem. A* **2000**, *104*, 4203.

23. Lednev, I. K.; Ye, T. Q.; Hester, R. E.; Moore, J. N. *J. Phys.Chem.* **1996**, *100*, 13338.
24. Lednev, I. K.; Ye, T. Q.; Matousek, P.; Towrie, M.; Foggi, P.; Neuwahl, F. V. R.; Umapathy, S.; Hester, R. E.; Moore, J. N. *Chem. Phys. Lett.* **1998**, *290*, 68.
25. Hirose, Y.; Yui, H.; Sawada, T. *J. Phys. Chem. A* **2002**, *106*, 3067.
26. Monti, S.; Orlandi, G.; Palmieri, P. *Chem. Phys.* **1982**, *71*, 87.
27. Cattaneo, P.; Persico, M. *Phys. Chem. Chem. Phys.* **1999**, *1*, 4793.
28. Biswas, N.; Umapathy, S. *J. Phys. Chem. A* **1997**, *101*, 5555.
29. Kurita, N.; Tanaka, S.; Itoh, S. *J. Phys. Chem. A* **2000**, *104*, 8114.
30. Pedersen, S.; Zewail, A. H. *Mol. Phys.* **1996**, *89*, 1455.